Numerical Investigation of Different Aerospike Nozzle Geometries with a Conventional Nozzle

Md. Zawadul Karim[*], Jagobandhu Some[*], Muhammad Sharif[*], Mohammad Mahdi Hasan[*]

[*] *Bangladesh Space Research and Remote Sensing Organization (SPARRSO), Dhaka, Bangladesh*

DOI: 10.29322/IJSRP.16.06.2026.p17413
https://dx.doi.org/10.29322/IJSRP.16.06.2026.p17413

Paper Received Date: 17th April 2026
Paper Acceptance Date: 19th May 2026
Paper Publication Date: 22nd June 2026

Abstract- This research shows a comparative numerical investigation of various aerospike nozzle configurations, including a traditional conical nozzle, under ideal flow conditions. The geometric contours of the full-spike, 40%-truncated, central-bleed truncated, hybrid aerospike nozzles, and the conical nozzle were numerically designed with a uniform expansion ratio. The nozzle geometries were subsequently analyzed using 2D axisymmetric CFD simulations in ANSYS Fluent with the k-ε turbulence model at an optimal nozzle pressure ratio of 47.64 to assess the impact on flow behavior, shock structure, thermal distribution, thrust performance, and specific impulse. The study indicates that the conventional conical nozzle is inefficient. In contrast, the full-spike nozzle offers better altitude compensation, with a maximum thrust of 9.99 kN and a specific impulse of 91.26 s. Among the truncated aerospike nozzles, the hybrid nozzle offers the best balance among aerodynamic effectiveness, geometric compactness, and structural feasibility, demonstrating its suitability for future space applications.

Index Terms- Computational Fluid Dynamics, Ideal Flow, Nozzle Pressure Ratio, Specific Impulse, Thrust.

I. Introduction

The propulsive figure of merits of a propulsion system is highly influenced by the geometric shape of the nozzle. It directs the high-speed exhaust gases produced during combustion by maximizing thrust and improving the aerodynamic performance. In earlier days, fixed-shaped conventional nozzles like C-D, bell, conical etc., were used for thrust generation. However, they are usually restricted to operating at their designated altitude and produce minimal performance for altitude change. Aerospike nozzle is an advanced nozzle that has a spike and lacks exterior walls, allowing the growth of pressure along the wall. It has the ability of altitude compensation while providing optimal performance. Additionally, the truncated versions of the aerospike nozzle have been under investigation for long periods due to their small plug length and reduced weight. This work mainly focuses on the variation of the numerical contribution of different aerospike nozzle contours with a conventional conical nozzle at the ideal flow condition to predict on its feasibility and performance capability for future space missions.

II. Literature Review

The aerodynamic and thermal characteristics of the engine are strictly governed by the nozzle geometry, which directly influences the exhaust gases and the conversion of thermal energy into thrust [1]. Fixed-geometry nozzles are the earliest and most widely used configurations in rocket propulsion. Conical nozzles were favored for their simple contour, ease of fabrication, and structural durability [2]. Although these pragmatic advantages exist, conventional nozzles are inherently sensitive to external pressure variations, which can lead to unwanted flow expansion and prevent the full utilization of available pressure energy [3].

Due to these limitations, further research was conducted to develop nozzle concepts that maintain improved performance over a wider range of operating conditions. The aerospike nozzle has been a major domain of investigation due to its altitude-compensating nature [4]. Unlike conventional nozzles with fixed divergent walls, the plug nozzle allows the exhaust plume to expand more adaptively to the environment [5]. Relatively short axial length and definite geometric arrangement have made them attractive for advanced rocket propulsion applications [6].

Researchers have studied aerospike nozzle design using theory, analysis, and computer models. Early work focused on identifying spike shapes that yielded nearly optimal thrust [7]. Later, these ideas were used to design axisymmetric spike nozzles [8]. As research continued, attention shifted to making practical changes to reduce the weight of full-length spikes [9]. Studies showed that by adjusting the inlet shape and shortening the plug [10], much of the aerodynamic benefit could be kept while making the nozzle shorter, lighter,

and simpler [11]. As a result, optimizing aerospike nozzle shapes, especially the spike contour and truncation ratio, remains an important area of research.

In addition to the full-length aerospike, several modified configurations have been explored to achieve improved balance between aerodynamic effectiveness and practical feasibility. Truncated spike nozzles have been studied as a means of reducing structural mass and manufacturing complexity whilst preserving acceptable thrust performance [12]. These studies show that the aerodynamic performance of aerospike nozzles depends not only on the general concept of external expansion but also strongly on detailed geometrical characteristics and configuration-specific design choices. [13].

Unlike previous studies that focus mainly on conventional nozzles such as C-D, bell, and conical, and on full-spike nozzles [14], this research provides a systematic comparison of the performance of 2D axisymmetric full, truncated, and hybrid aerospike configurations with that of a conventional conical nozzle, highlighting the importance of using such nozzles for space missions. Even though aerospike nozzles pose practical difficulties owing to their complicated structure, which depends on their dimensional configuration [15]. By comparing conventional and advanced nozzle configurations within a unified computational framework, this study aims to clarify which configuration offers the optimal trade-off for future propulsion applications.

III. Analytic and Numerical Design of the Aerospike Nozzle

The geometric contour of the full-spike nozzle was developed using Angelino's approximate method [8] in combination with the isentropic flow relations, along with modified truncated nozzles [16]. In this work, the flow at the nozzle end was assumed to be uniform and parallel to the nozzle back and evaluated using equation (1), and the exit Mach number was determined using equation (2) [17].

$$\text{Thruster angle, } \theta_t = \left(\sqrt{\frac{\gamma+1}{\gamma-1}}\tan^{-1}\sqrt{\frac{\gamma-1}{\gamma+1}\times\left(M_e{}^2-1\right)}\right)-\tan^{-1}\left(\sqrt{M_e{}^2-1}\right) \ldots\ldots (1)$$

$$\text{Exit Mach Number, } M_e = \sqrt{\left[\left(\frac{P_e}{P_t}\right)^{\frac{\gamma-1}{-\gamma}}-1\right]\times\frac{2}{\gamma-1}} \ldots\ldots (2)$$

To achieve a nozzle flow parallel to the nozzle axis, the optimal expansion ratio was obtained using equation (3), while the corresponding exit nozzle radius was obtained using equation (4).

$$\text{Expansion Ratio, } \varepsilon = \frac{1}{M_e}\left[\frac{2}{\gamma+1}\left(1+\frac{\gamma-1}{2}M_e^2\right)\right]^{\frac{\gamma+1}{2(\gamma-1)}} \ldots\ldots (3)$$

$$\text{Exit Radius, } r_e = \sqrt{\frac{\left(\frac{r_t^2\varepsilon}{\cos(\theta_t)}-r_b^2\right)}{\frac{\varepsilon}{\cos(\theta_t)}-1}} \ldots\ldots (4)$$

The throat and exit areas were determined using Angelino's approximation approach, as described by equations (5) and (6).

$$\text{Throat area, } A_t = \frac{\pi(r_e^2-r_t^2)}{\cos(\theta_t)} \ldots\ldots (5)$$

$$\text{Exit area, } A_e = A_t\varepsilon \ldots\ldots (6)$$

The characteristic line segments used to generate the spike contour were computed in the axial and radial directions using equations (7) and (8) [18].

$$x = l\cos(\mu + \theta_t - \theta_a) \dots\dots (7)$$

$$y = l\sin(\mu + \theta_t - \theta_a) \dots\dots (8)$$

The input parameters adopted using the equations and isentropic flow properties for the full-spike contour generation were selected to satisfy the required parallel-flow condition and are listed in Table 1.

Table 1. Geometric Parameters for Full Spike Nozzle Contour

Input Parameters	Numerical Value
Throat Radius	50 mm
Throat Height	5.41 mm
Ambient Pressure	101325 Pa
Exit Radius	52.35 mm
Base Radius	0 (Due to full spike nozzle)
Specific Heat Ratio	1.4
Thruster Angle	53.01 Degree

Subsequently, an optimized MATLAB algorithm was used with the input parameters to generate the basic full-spike nozzle contour with a design pressure ratio of 47.64 and an expansion ratio of 5, as shown in Fig. 1. The resulting contour data were then imported into SolidWorks to create the full-spike geometry. Based on this baseline design, three modified configurations were subsequently developed: a 40%-truncated aerospike nozzle, a central-bleed aerospike nozzle, and a hybrid aerospike nozzle, as illustrated in Figs. 2–5.

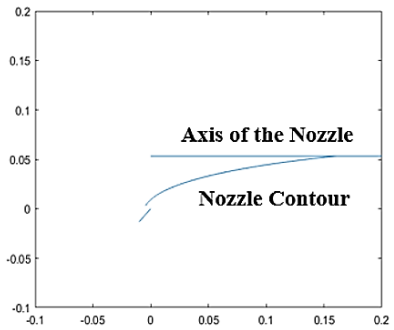

Fig. 1. Full spike nozzle contour

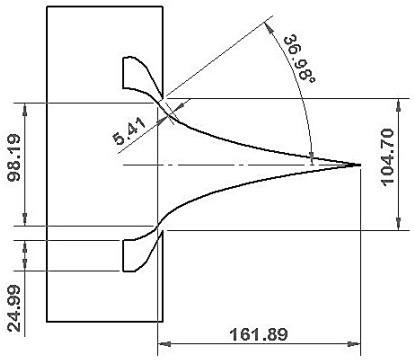

Fig. 2. Full spike nozzle geometry

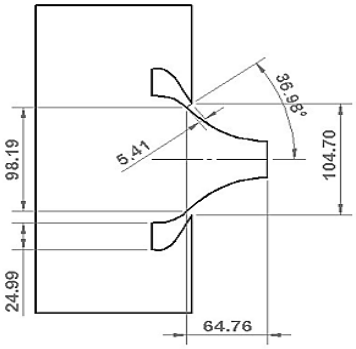

Fig. 3. 40% truncated aerospike nozzle geometry

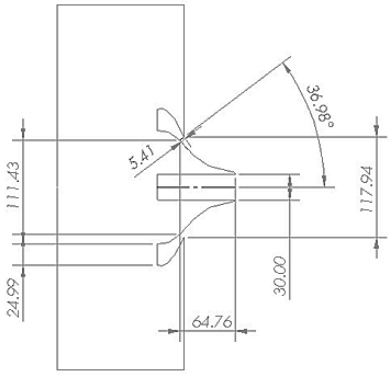

Fig. 4. Truncated central bleed aerospike nozzle geometry

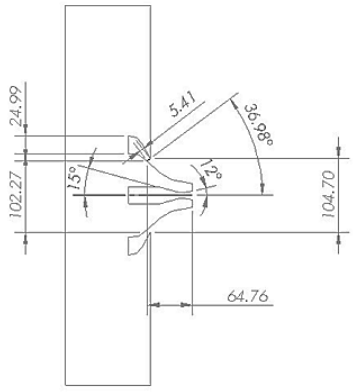

Fig. 5. Truncated hybrid aerospike nozzle geometry

IV. Analytic and Numerical Design of the Conical Nozzle

The geometric contour of the conical nozzle was generated using isentropic flow relations and Prandtl–Meyer-based compressible-flow considerations with the same expansion ratio of the spike nozzle [2]. The model was then developed in SolidWorks, as shown in Fig. 6.

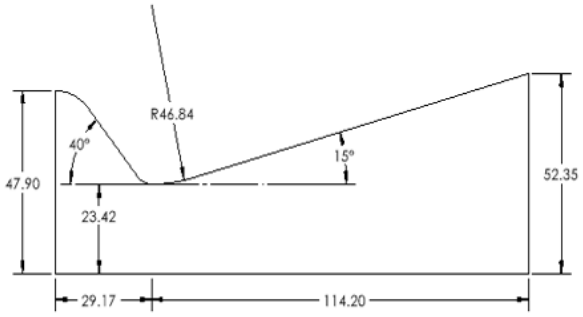

Fig. 6. Conical nozzle geometry

V. Computational Fluid Dynamics Analysis

A. Computational Domain Design and Meshing

CFD simulations were performed in ANSYS Fluent (2025) to investigate the flow structure, shock patterns, and aerodynamic behavior of the nozzle designs. For each case, the computational domain was defined and then divided using structured meshing, with face and edge sizes specified. Finer mesh was used near the nozzle wall, throat, and exhaust plume, while a coarser mesh was used farther from the nozzle. Additional refinement beyond the adopted mesh density produced negligible visible changes in the primary flow characteristics; therefore, the selected mesh was considered adequate for the present comparative analysis. Figs. 7-11 show the meshed domains for the conical, full-spike, truncated, central-bleed, and hybrid aerospike nozzles.

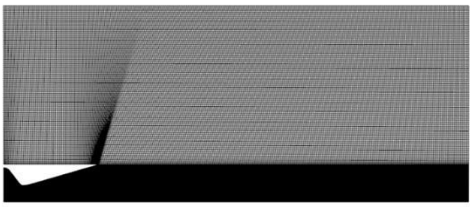

Fig. 7. Conical nozzle meshed domain

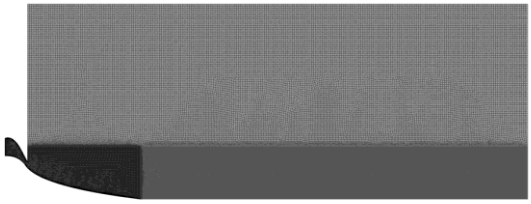

Fig. 8. Full spike nozzle meshed domain

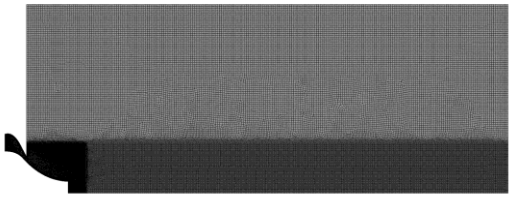

Fig. 9. 40% Truncated aerospike nozzle meshed domain

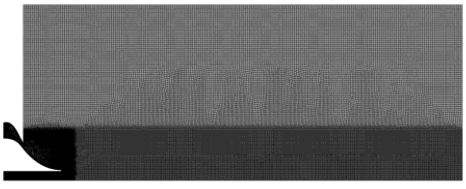

Fig. 10. Truncated central bleed aerospike nozzle meshed domain

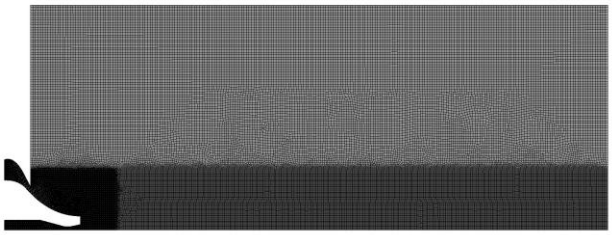

Fig. 11. Truncated hybrid aerospike nozzle meshed domain

B. CFD Setup and Boundary Conditions

A density-driven coupled solver was used to capture compressible flow. All simulations were conducted under steady-state conditions. The energy equation was included to account for thermal effects. The Sutherland viscosity model and the k-ε turbulent flow model boosted predictions of turbulent flow and shock boundary-layer interactions. Table 2 summarizes the boundary conditions for the ideal operating condition.

Table 2. Boundary Conditions

Nozzle Pressure Ratio: 47.64
Inlet Total Pressure: 4827123 Pascal
Initialization Pressure: 4710000 Pascal
Inlet Total Temperature: 879 K
Pressure Outlet: 101325 Pascal
Outlet Total Temperature: 288.16 K
Operating Pressure: 0 Pa
Far-field Boundary: Wall

VI. Result and Discussion

All the nozzle configurations were analyzed under the optimal flow condition, where the pressure at the nozzle outlet matches the surrounding pressure. The validation was performed using analytical methods. For the analytical process, the exit parameters, such as – exit Mach number and exit velocity, have been obtained from the isentropic flow properties. Using this design ratio and equations (9), (10), and (11), the exit Mach number and velocity were obtained and compared with the simulated exit properties of the full spike nozzle. The percentage error was found to be less than 5%, indicating good agreement between the analytical and numerical results. This low deviation confirms the reliability of the numerical methodology adopted in the present study.

$$\text{Exit Mach Number, } M_e = \sqrt{\left[\left(\frac{P_e}{P_t}\right)^{\frac{\gamma-1}{-\gamma}} - 1\right] \times \frac{2}{\gamma - 1}} \ldots\ldots (9)$$

$$\frac{T_e}{T_t} = \left(1 + \frac{\gamma - 1}{2} \times M_e^2\right)^{-1} \ldots\ldots (10)$$

$$V_e = M_e \times \sqrt{\gamma \times R \times T_e} \ldots\ldots (11)$$

The analysis provided important contours, including Mach, velocity, and density contours, along with a static pressure chart. etc., to understand the impact of spike nozzles. The velocity contours indicate clear differences in flow behavior, shock structure, and aerodynamic performance among the nozzle configurations. The conical nozzle produces a strongly under expanded jet with pronounced shock cells, resulting in significant shock losses. In contrast, the full-spike nozzle produces a uniform velocity field due to external expansion along the spike, thereby securing superior pressure adaptation. The truncated nozzle has a slight reduction in peak velocity. The incorporation of a central bleed into the 40%-truncated aerospike improves base pressure and wake stability, thereby weakening shock patterns and yielding smoother axial-velocity maps. Among the truncated configurations, the 40% truncated hybrid conical aerospike nozzle exhibits much more favorable flow characteristics, with the weakest shock patterns and an almost uniform axial velocity distribution, showing a better balance between aerodynamic effectiveness, flow steadiness, and geometric compactness, as shown in the Figs. 12-16.

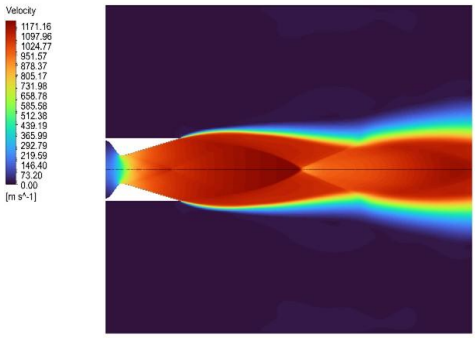

Fig. 12. Conical nozzle velocity contour

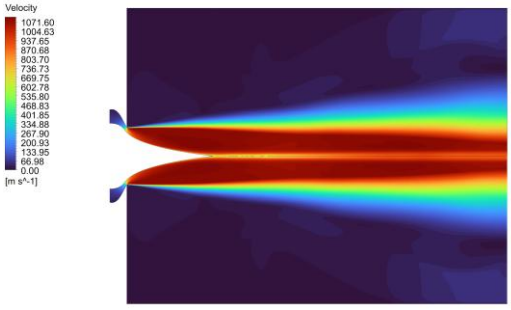

Fig. 13. Full spike nozzle velocity contour

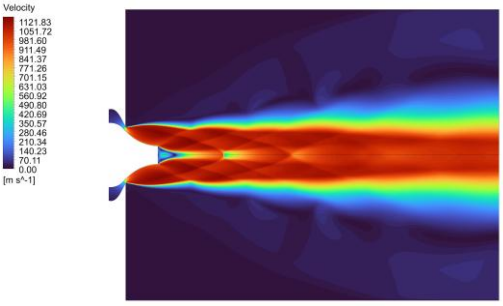

Fig. 14. 40% Truncated aerospike nozzle velocity contour

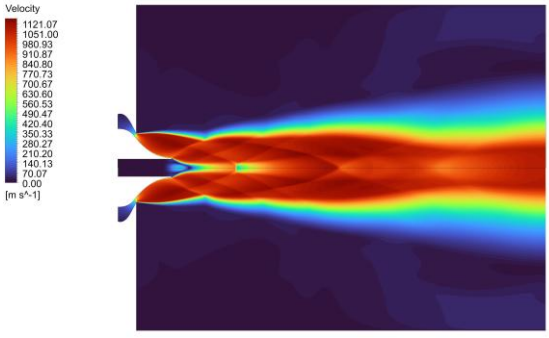

Fig. 15. Truncated central bleed aerospike nozzle velocity contour

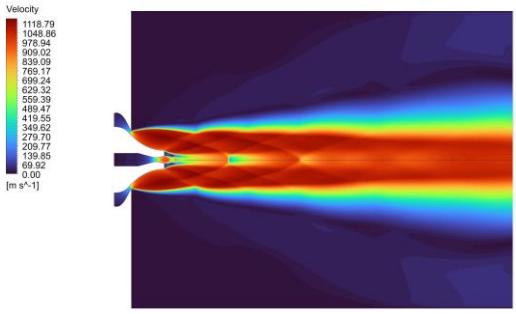

Fig. 16. Truncated hybrid aerospike nozzle velocity contour

The thermal contours also reveal the clear differences among these nozzle configurations. As shown in Fig. 17, the conical nozzle shows relatively high thermal gradients due to shock-induced heating, whereas the full spike shown in Fig. 18 has smoother temperature distributions with weaker shock effects and improved energy expansion characteristics. However, the 40% truncated spike nozzle in Fig. 19 develops a localized high temperature region at the nozzle end due to flow separation, though the thermal field remains more uniform than the conical nozzle, with a certain improvement including the central bleed shown in Fig. 20. The hybrid nozzle has an optimal thermal nature with lowest temperature peaks, smooth axial decay, with enhanced flow stability as shown in Fig. 21.

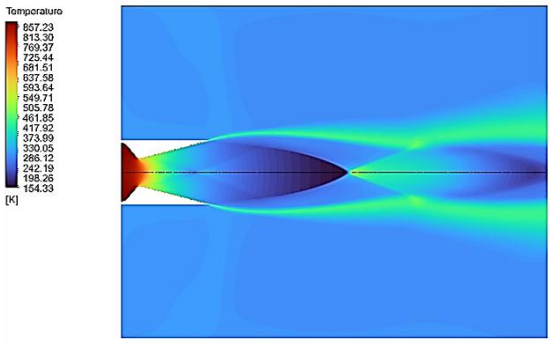

Fig. 17. Conical nozzle temperature contour

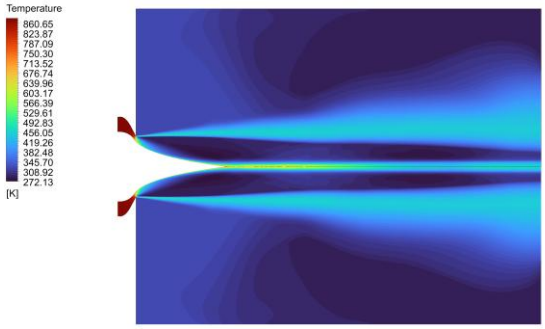

Fig. 18. Full spike nozzle temperature contour

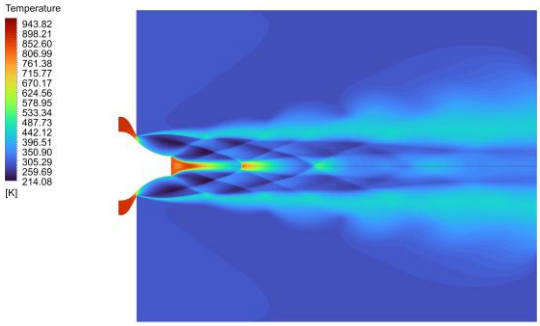

Fig. 19. 40% Truncated aerospike nozzle temperature contour

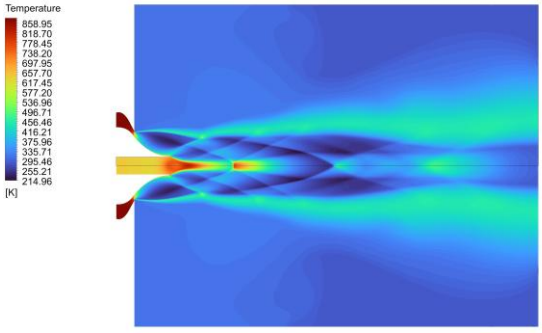

Fig. 20. Truncated central bleed aerospike nozzle temperature contour

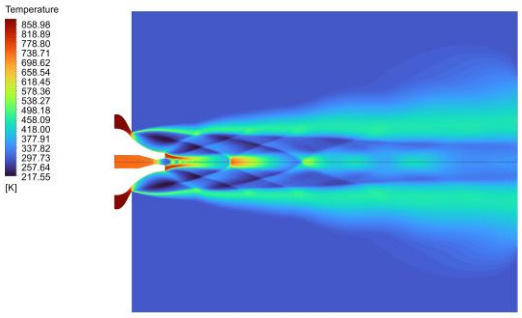

Fig. 21. Truncated hybrid aerospike nozzle temperature contour

Moreover, the primary propulsive performance indicators examined are mass flow rate, thrust force, and specific impulse. Table 3 compares these properties for the nozzles at NPR of 47.64.

Table 3. Comparative Analysis of Propulsive Performance of the Nozzles

Nozzle Type	Mass Flow Rate (kg/s)	Thrust (kN)	Specific Impulse (s)
Conical	9.03	9.35	88.62
Full-Spike	11.16	9.99	91.26
40% Truncated Spike	10.83	9.46	89.01
Truncated Central Bleed Aeropike	10.83	9.48	89.21
Truncated Hybrid Aerospike	10.83	9.51	89.45

As presented in Table 3, the full spike nozzle achieved the highest thrust and specific impulse among all the configurations investigated, which is consistent with the well-known performance advantages of aerospike nozzles. Among the truncated designs, the hybrid aerospike nozzle provided the best overall balance in terms of mass flow rate, thrust, and specific impulse, producing performance close to that of the full aerospike nozzle.

VII. CONCLUSION

This work proves that while the conventional fixed-geometry nozzle is simple, it suffers significant shock losses and limited efficiency when operating outside its design range. In contrast, the full spike nozzle and its truncated versions perform better at high altitudes by providing higher thrust and specific impulse. These outcomes establish a solid foundation for creating advanced, optimized nozzles that overcome geometric and structural intricacies with future scopes including – 3D CFD analysis, extended over-expanded and under-expanded flow analysis, small- and large-scale experimental validation, ML-based optimization, and finally manufacturing feasibility for future inclusion in space missions

ACKNOWLEDGMENT

The author gratefully acknowledges the support from the Bangladesh Space Research and Remote Sensing Organization (SPARRSO) to conduct this research work.

REFERENCES

[1] G. P. Sutton and O. Biblarz, *Rocket Propulsion Elements*, 9th ed. Hoboken, NJ, USA: John Wiley & Sons, Inc., 2017, pp. 2–48.

[2] S. Khare and U. K. Saha, "Rocket nozzles: 75 years of research and development," *Sādhanā*, vol. 46, no. 2, pp. 1–22, 2021.

[3] I. R. Cardenas, S. Laín, and O. D. Lopez, "A review of aerospike nozzles: Current trends in aerospace applications," *Aerospace*, vol. 12, no. 6, 2025.

[4] G. Hagemann, H. Immich, T. V. Nguyen, and G. E. Dumnov, "Advanced rocket nozzles," *Journal of Propulsion and Power*, vol. 14, no. 5, pp. 610–654, 1998.

[5] K. Naveen Kumar, M. Gopalsamy, D. Antony, R. Krishnaraj, and C. B. V. Viswanadh, "Design and optimization of aerospike nozzle using CFD," *IOP Conference Series: Materials Science and Engineering,* vol. 247, 2017.

[6] G. I. Evans, "Modern engineering for design of liquid-propellant rocket engines—Revised edition," *The Aeronautical Journal*, vol. 98, no. 976, p. 232, 1994.

[7] G. V. R. Rao, "Spike nozzle contour for optimum thrust," *Planetary and Space Science*, vol. 4, pp. 90–108, 1961.

[8] G. Angelino, "Approximate method for plug nozzle design," *AIAA Journal*, vol. 2, no. 10, pp. 1824–1855, 1964.

[9] G. Hagemann, H. Immich, and M. Terhardt, "Flow phenomena in advanced rocket nozzles—The plug nozzle," in *Proc. 34th AIAA/ASME/SAE/ASEE Joint Propulsion Conference and Exhibit*, Cleveland, OH, USA, Jul. 11–15, 1998.

[10] G. R. Johnson, H. D. Thompson, and J. D. Hoffman, "Design of maximum thrust plug nozzles with variable inlet geometry," *Computers & Fluids*, vol. 2, no. 2, pp. 164–192, 1974.

[11] J. Ruf and P. McConaughey, "A numerical analysis of a three-dimensional aerospike," *Proc. 33rd Joint Propulsion Conference and Exhibit*, Seattle, WA, USA, Jul. 6–9, 1997.

[12] G. Sujesh, G. Hrishika, P. S. Pravya, S. Satheesan, and K. S. Surya, "Performance analysis of truncated aerospike nozzles: A study on thrust enhancement and weight reduction," *International Journal of Research and Analytical Reviews*, vol. 12, no. 1, pp. 676–682, 2025.

[13] C. H. Wang, Y. Liu, and Y. F. Liao, "Studies on aerodynamic behavior and performance of aerospike nozzles," *Chinese Journal of Aeronautics*, vol. 19, no. 1, pp. 1–9, 2006.

[14] G. M. J. Alam, M. Z. Karim, S. J. Santho, and M. A. Lopa, "Comparison of performance between aerospike and bell nozzle under uniform expansion ratio for aerospace applications," *AIP Conf. Proc.,* vol. 3451, 2026.

[15] S. Soman, A. Suryan, P. P. Nair, M. Ritter, and H. D. Kim, "Study on control of unsteadiness and flow asymmetry in linear aerospike nozzles," *Journal of Spacecraft and Rockets*, vol. 60, no. 1, pp. 1–12, 2023.

[16] S. Farrag, *Aerospike Nozzle Design and Analysis*. Istanbul, Turkey: Istanbul Technical University, Institute of Science and Technology, 2020.

[17] J. D. Anderson, *Fundamentals of Aerodynamics*, 5th ed. New York, NY, USA: McGraw-Hill Education, 2016, pp. 1047–1051.

[18] T. J. Mueller and W. P. Sule, "Basic flow characteristics of a linear aerospike nozzle segment," *Proc. Winter Annual Meeting of the American Society of Mechanical Engineers*, New York, NY, USA, Nov. 26–30, 1972.

AUTHORS

First Author – Md. Zawadul Karim, Junior Research Fellow, SPARRSO*;* Email address: zawadulkarim07@gmail.com
Second Author – Jagobandhu Some, Senior Engineer, SPARRSO*;* Email address: jagobandhusome@gmail.com
Third Author – Muhammad Sharif, Assistant Engineer, SPARRSO; Email address: sharif191294@gmail.com
Fourth Author - Mohammad Mahdi Hasan, Senior Scientific Officer, SPARRSO; Email address: mahdi.sparrso@gmail.com

Correspondence Author – Md. Zawadul Karim, zawadulkarim07@gmail.com